HHS Public Access

Author manuscript

ACS Appl Bio Mater. Author manuscript; available in PMC 2021 May 04.

Published in final edited form as:

ACS Appl Bio Mater. 2021 February 15; 4(2): 1450–1460. doi:10.1021/acsabm.0c01336.

Targeted polymeric nanoparticles for drug delivery to hypoxic, triple-negative breast tumors

Babak Mamnoon[1], **Jagadish Loganathan**[1], **Matthew I. Confeld**[1], **Nimesha De Fonseka**[1], **Li Feng**[1], **Jamie Froberg**[2], **Yongki Choi**[2], **Daniel M. Tuvin**[3], **Venkatachalem Sathish**[1], **Sanku Mallik**[1,*]

[1]Department of Pharmaceutical Sciences, North Dakota State University, Fargo, North Dakota 58102, United States.

[2]Department of Physics, North Dakota State University, Fargo, North Dakota 58102, United States.

[3]Sanford Broadway Clinic, Fargo, North Dakota 58102, United States.

Abstract

High recurrence and metastasis to vital organs are the major characteristics of triple-negative breast cancer (TNBC). Low vascular oxygen tension promotes resistance to chemo- and radiation therapy. Neuropilin-1 (NRP-1) receptor is highly expressed on TNBC cells. The tumor-penetrating iRGD peptide interacts with the NRP-1 receptor, triggers endocytosis and transcytosis, and facilitates penetration. Herein, we synthesized a hypoxia-responsive diblock PLA–diazobenzene–PEG copolymer and prepared self-assembled hypoxia-responsive polymersomes (Ps) in an aqueous buffer. The iRGD peptide was incorporated into the polymersome structure to make hypoxia-responsive iRGD-conjugated polymersomes (iPs). Doxorubicin (DOX) was encapsulated in the polymersomes to prepare both targeted and non-targeted hypoxia-responsive polymersomes (DOX-iPs and DOX-Ps, respectively). The polymeric nanoparticles released less than 30% of their encapsulated DOX within 12 hours under normoxic conditions (21% oxygen), whereas under hypoxia (2% Oxygen), doxorubicin release remarkably increased to over 95%. The targeted polymersomes significantly decreased TNBC cells' viability in monolayer and spheroid cultures under hypoxia compared to normoxia. Animal studies displayed that targeted polymersomes significantly diminished tumor growth in xenograft nude mice. Overall, the targeted polymersomes exhibited potent anti-tumor activity in monolayer, spheroid, and animal models of TNBC. With further developments, the targeted nanocarriers discussed here might have the translational potential as drug carriers for the treatment of TNBC.

Graphical Abstract

[*]**Corresponding Author**. Sanku Mallik, Phone: 701-231-7888, Fax: 701-231-7831. sanku.mallik@ndsu.edu.

Appendix A. Supplementary data

The following is Supplementary data to this research:

^{1}H NMR spectrum of the hypoxia-responsive polymer PLA_{8500}–diazobenzene–PEG_{2000}, ^{13}C NMR spectrum of the hypoxia-responsive polymer PLA_{8500}–diazobenzene–PEG_{2000}, GPC in THF of the hypoxia-responsive polymer PLA_{8500}–diazobenzene–PEG_{2000}, MALDI-TOF mass spectrum of the synthesized iRGD peptide, circular dichroism (CD) spectrum of the synthesized iRGD peptide, a calibration curve of doxorubicin hydrochloride solution, polymersome stability at 4 °C.

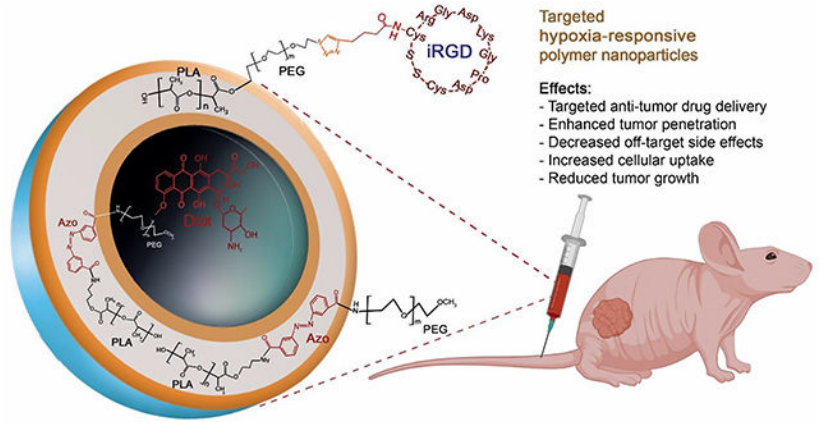

Keywords

Hypoxia; Nanotechnology; Polymersomes; Targeted Drug Delivery; Nanoparticles

1. Introduction

Breast cancer is a challenging disorder for women, regardless of the treatment strategy used.[1] A high recurrence rate and metastasis to different organs (e.g., lung, bone, liver, and lymph nodes) contribute to adverse outcomes.[2] Metastatic breast cancer claims about 40,000 lives in the US annually.[3] Triple-negative breast cancer (TNBC) is marked by the loss of all biomarker expression[4] and includes about 15% of all diagnosed breast malignancies.[5] Based on the gene expression profiles, there are four subtypes of TNBC.[6] Effective therapies are available for the estrogen, progesterone, and human epidermal growth factor receptor-positive subtypes. However, no promising treatment exists for TNBC other than systemic chemotherapy.[7] This is partially due to rapid cell proliferation and inadequate blood flow, which creates a low oxygen concentration (hypoxia) in tumors.[8] Notably, hypoxia is a primary driver of metastasis and aggressiveness in TNBC, which hinders treatment.[9–11]

Due to the lack of specific targeting, chemotherapeutic drugs for TNBC inflict severe damage to healthy tissues. Besides, low solubility, decreased bioavailability, and accelerated clearance of drugs from the bloodstream make it challenging to achieve the desired clinical outcomes.[12] To address these problems, nanotechnology has emerged as a rapidly developing field to design drug carriers for TNBC treatment.[13,14] Drugs encapsulated in nanocarriers have several advantages compared to the free molecules. For instance, polymeric nanoparticles help increase lipophilic drugs' solubility by carrying these drugs within their bilayer.[15–18] Polyethylene glycol (PEG) on the outer layer extends the nanoparticles' circulation time and allows accumulation into the cancer tissues through enhanced permeability and retention (EPR) effect.[19] Nanoscale carriers with targeting moieties for the overexpressed surface receptors target the disease site, thus minimizing off-target side effects.[20,21] In addition, stimuli-responsive nanoparticles respond to specific triggers for releasing anticancer drugs only in the presence of a stimulus.[22]

Polymersomes are nanoparticles prepared from amphiphilic copolymers. Several properties render polymersomes more advantageous than other nanoparticles, including membrane stability, the tunable molecular weight of the polymers, ligand conjugation capacity, and more.[23,24] Hydrophobic molecules are encapsulated within the polymer bilayer, whereas hydrophilic drugs are incorporated into the aqueous core of the polymersomes, thereby carrying both types of drugs simultaneously.[25]

The tumor-penetrating iRGD peptide (CRGDKGPDC) contains the RGD motif for specific interactions with the overexpressed $\alpha_v\beta_3$ integrins on endothelial cancer cells.[26] Subsequent cleavage of iRGD peptide exposes the CendR (RGDK) motif with a higher binding affinity to the neuropilin-1 (NRP-1) receptor. This ligand-receptor binding promotes transcytosis and endocytosis, leading to tumor penetration.[27] Hence, surface conjugation of iRGD peptide to the drug-encapsulated polymersomes allows them to penetrate solid tumors [28] (Figure 1).

Doxorubicin (DOX) is a common anthracycline drug used for treating various cancers, particularly TNBC.[8,29] DOX can be encapsulated into biocompatible nanocarriers to increase therapeutic index and sustained release.[30] In this study, we synthesized DOX-encapsulated, iRGD-conjugated, hypoxia-responsive, polymersomes (DOX-iPs) as targeted drug delivery vehicles to deliver DOX into solid tumors of TNBC. The targeted polymersomes offered here are dual-functional nanoparticles that bind specifically to the surface NRP-1 receptors and translate into TNBC cells. Then, the diazobenzene linker of the PLA-PEG polymer undergoes reduction within hypoxia, disintegrates the polymersome membrane, and releases encapsulated DOX in the tumor microenvironment. We also prepared non-targeted polymersomes (DOX-Ps) to evaluate their efficacy along with targeted polymersomes.

2. Materials and Methods

2.1. Chemicals

The amino acids were purchased from Alfa Aesar. DPPE-lissamine rhodamine lipid dye was obtained from Avanti Polar Lipids. $mPEG_{2000}$-NH_2 was bought from Biochempeg. All other chemicals for polymer synthesis were purchased from Millipore Sigma. The complete cell culture medium was obtained from VWR International. The antibiotic-antimycotic (Penicillin-Streptomycin-Amphotericin B) solution was purchased from Corning.

2.2. Synthesis and characterization of copolymers and targeting peptide

The PLA_{8500}-Azo-PEG_{2000} polymer was synthesized in our laboratory, as previously reported.[8] The ^1H NMR, ^{13}C NMR, and gel permeation chromatography (GPC) were used to analyze the final product (Supporting Information, Figures S1–S3). As previously reported, a peptide synthesizer (Liberty Blue) was used for synthesizing Hex-iRGD in our laboratory.[17] The product (145 mg, 64%) was characterized by circular dichroism and mass spectrometry (Supporting Information, Figures S4–S5).

2.3. Synthesis of PLA_{8500}–PEG_{2000}–iRGD polymer

The PLA_{8500}–PEG_{2000}–N_3 polymer was synthesized in our laboratory, as previously reported.[31] [2+3]-cycloaddition reaction was carried out for conjugating Hex-iRGD to PLA_{8500}–PEG_{2000}–N_3 polymer, as previously reported.[17] The lyophilized product was freeze-dried (yield: 50%) and characterized by circular dichroism spectroscopy (Supporting Information, Figure S5).

2.4. Preparation of the polymersomes encapsulating doxorubicin

The fluorescent lipid DPPE-N-lissamine rhodamine (LR, 5%), PLA_{8500}-Azo-PEG_{2000} polymer (85%), and PLA_{8500}–PEG_{2000}–iRGD (10%) were used for preparing targeted doxorubicin-encapsulated polymersomes (DOX-iPs). LR (5%) and PLA_{8500}-Azo-PEG_{2000} polymer (95%) were used to make doxorubicin-encapsulated polymersomes (non-targeted polymersomes, DOX-Ps). Doxorubicin encapsulated polymersomes were prepared using the pH gradient method.[29] The method and chemicals used to prepare polymersomes were previously reported.[8]

2.5. Preparation of plain polymersomes

Plain (HEPES buffer-encapsulated) nanoparticles were made from the PLA_{8500}-Azo-PEG_{2000} polymer (95%) and LR dye (5%). Briefly, LR was air-dried to make a thin layer film. PLA_{8500}-Azo-PEG_{2000} polymer (100 μL) was mixed with the dried LR and added dropwise into 1000 μL 25 mM HEPES buffer (pH 7.4) and evaporated for 45 minutes. Subsequently, the mixture was sonicated for 1 hour and filtered by Sephadex G100 column. Plain polymersomes were the control for the cell cytotoxicity studies.

2.6. Characterization

The charge and size of the polymersomes were measured by Dynamic Light Scattering (DLS) instrument (Malvern Zetasizer). All samples were measured five times, and the average was recorded.

Nanoparticle solutions (10 μL, 1 mg/mL) were dried by nitrogen flow. A microscope (NT-MDT NTEGRA AFM) was employed for acquiring AFM images. Samples were prepared for transmission electron microscopic (TEM) images based on a reported protocol.[8]

2.7. Release studies

The release kinetics of the nanoparticles was carried out by preparing a mixture of targeted polymersomes, NADPH, and liver microsomes under hypoxic (2% oxygen) and normoxic (21% oxygen) conditions according to previously reported protocol from our laboratory.[8] The loading content and encapsulation efficiency of the drug in the vesicles were calculated by measuring absorbance at 480 nm.[32]

2.8. Cell culture

The MDA-MB-231 cells were purchased from American Type Culture Collection (Manassas, VA) and cultured as recommended by the vendor. For the normoxic conditions, cells were grown in an incubator at 37 °C containing 5% CO_2 and 21% oxygen. For the

hypoxic conditions, cells were incubated in a hypoxia chamber (Biospherix C21) with 5% CO_2 and 2% oxygen at 37 °C.

2.9. Neuropilin-1 protein expression

The TNBC cells were seeded (2.5×10^5 cells/well) in cell culture plates and incubated in normoxic conditions. When the cells reached around 40 to 50% confluence, a set of plates were moved to the hypoxia chamber (2% oxygen). The cells were then incubated in both hypoxic and normoxic chambers, and their protein was collected after 24 hours. The whole-cell lysates were analyzed using 10% SDS polyacrylamide gel electrophoresis. Proteins were transferred on PVDF membranes before incubation with NRP-1 (Abcam) and β-Actin (Applied Biological Materials) primary antibodies. Protein bands were detected by imaging the membrane, and densitometry analysis was carried out by Image Studio v.5.2 software.

2.10. Cellular uptake studies

The cells were seeded (5,000 cells/well) in two 12-well tissue culture plates and incubated under 5% CO_2. When the cells reached 80% confluence, they were washed with 1X PBS and replenished with fresh cell culture media. Then, one of the plates was moved to the hypoxia chamber (2% oxygen) for one doubling time before starting the experiments. The cells in both plates were treated with iRGD-conjugated and non-conjugated polymersomes (targeted and non-targeted treatments, respectively, 20 μL each) for three hours. The plates were then washed three times with PBS, and the cell nuclei were stained with DAPI (NucBlue, Invitrogen). The images were taken by a Leica fluorescence microscope and analyzed by the NIH ImageJ (version: 1.52a) software.

2.11. Cell viability and cytotoxicity in monolayer cultures

The cells were seeded (5,000 cells/well) in the plates and grown 24 hours. The wells containing the cells were categorized into five treatments: HEPES-buffer encapsulated polymersomes, non-targeted polymersomes (DOX-Ps), targeted polymersomes (DOX-iPs), free DOX, and control (only HEPES buffer). In these experiments, 1, 2, and 4 μM of free DOX and the same amounts of drug-encapsulated polymersomes were used for 72 hours under hypoxic and normoxic conditions. For the cytotoxicity study, the cells were incubated with different concentrations of plain polymersomes (20 to 100 μg/mL). The cytotoxicity was measured after 4 hours by recording the fluorescence (excitation at 560 nm and emission at 595 nm).

2.12. Three-dimensional cytotoxicity studies

The spheroids were prepared using a Nanoshuttle three-dimensional cell culture kit (Greiner Bio-one). The NanoShuttle nanoparticles (200 μL) were added into 80–90% confluent MDA-MB-231 cells for magnetizing the cells overnight. The cells were dislodged, counted, and 20,000 cells were transferred into each well. The plates were laid on top of magnetic spheroid drives for 15 minutes to form spheroids and incubated for 24 hours. The wells were then categorized into five treatments and incubated for 72 hours in hypoxia and normoxia with three different doxorubicin concentrations (1, 2, and 4 μM). The spheroids were then

washed with PBS, transferred to new plates for growing 24 hours. Subsequently, the cytotoxicity was determined (same as monolayer cell viability assay).

2.13. *In vivo* toxicity and anti-tumor efficacy

The anti-tumor efficacy of the polymersomes was evaluated on tumor-bearing mouse models, following an approved IACUC protocol. The MDA-MB-231 cell suspension (10^6 cells per mouse) was mixed in Matrigel (Corning) at a 1:1 ratio (total 200 μL) and subcutaneously injected into the 8-week-old female athymic nude mice (Envigo). Three weeks after injection, 30 mice with a tumor volume ranging from 50–80 mm^3 were randomly divided into five treatment groups. The treatment groups were vehicle, free DOX, polymersomes, non-targeted, and targeted nanoparticles. The control and polymersome-only groups received saline and polymersomes, respectively. The other 3 groups received 5 mg DOX/kg dose. All treatments were given twice per week for four weeks. The body weights and tumor volumes were evaluated once every three days. Two weeks after the treatment ended, all mice were euthanized, the tumors were excised, and weighed. The vital organs were dissected and fixed in 10% formalin for histological evaluation.

2.14. *In vivo* biodistribution

Tumor-bearing female athymic nude mice were i.v. injected with iRGD-polymersomes containing lissamine rhodamine fluorescent dye. The mice were then euthanized after 3 and 8 hours; the organs (lung, liver, and kidney) were excised and imaged. The fluorescence integral density of accumulated polymersomes in each organ tissue was analyzed.

2. 15. Statistical analysis

The statistical analyses were all processed using Origin software (Origin 9.3, Northampton, Massachusetts) and presented as mean ± SEM. The significant statistical difference between normoxic and hypoxic conditions within treatment groups was evaluated by ANOVA.

3. Results and Discussion

3.1. Synthesis and characterization of polymersomes

Hypoxia contributes to the overall progression, migration, and invasion of TNBC and other solid tumors.[33] We synthesized PLA_{8500}-Azo-PEG_{2000} polymer with a hypoxia-responsive diazobenzene linker (Scheme 1 and Supporting Information, Figures S1, and S2), which self-assembles into polymersomes under appropriate conditions.

The polydispersity index was calculated from Gel Permeation Chromatography to be 1.17 (Supporting Information, Figure S3). The surface PEG groups increase circulation time and the amount of polymersomes in cancerous tissue microenvironment by EPR effect.[16] The alkyne functional group on hexynoic acid was used for the conjugation of iRGD peptide to the azide (N_3) functional group of PLA_{8500}–PEG_{2000}–N_3 polymer (Scheme 2). This peptide conjugation with the polymer was evaluated by circular dichroism spectroscopy (Supporting Information, Figure S5). We actively encapsulated doxorubicin into the nanoparticles, while unencapsulated doxorubicin was separated by passing the sample through a gel filtration column. A standard curve was plotted by measuring doxorubicin absorption as a function of

concentration (Supporting Information, Figure S6). The encapsulation efficiency and loading of the non-targeted polymersomes were 51% and 9 weight percent, and for the targeted polymersomes were 63% and 11 weight percent, respectively. These polymersomes were stable over 8 weeks at 4 °C (Supporting Information, Figure S7).

The synthesized PLA_{8500}–PEG_{2000}–iRGD conjugate was then incorporated into the polymeric nanoparticles to prepare doxorubicin encapsulated hypoxia-responsive iRGD-conjugated polymersomes (DOX-iPs). The iRGD peptide on the polymersome first targets $\alpha_v\beta_3$ and $\alpha_v\beta_5$ integrins on the cells. Subsequent enzymatic cleavage exposes the CendR (RGDK) motif to interact with the NRP-1 receptors, cellular internalization, and endocytic transcytosis.[34] The size, charge, and polydispersity index (PDI) of the nanoparticles were measured by dynamic light scattering, DLS (Figure 2A, 2B, Table 1), and the spherical shape was confirmed by atomic force microscopic (AFM) imaging (Figure 2C, 2D). The nanoparticles' average size significantly changed in hypoxic conditions (Figure 2A S8, Table 1). Targeted vesicles indicated larger diameters because of the conjugation of the iRGD peptide. Figure 2B, S9, and Table 1). The slightly positive ζ potential almost remained consistent within all conditions for non-targeted and targeted polymersomes (Table 1).

3.2. Release studies in hypoxia and normoxia

Solid tumors have an environment that is rich in reducing agents.[35] The diazobenzene moieties in the polymers' structure undergo a four-electron reduction reaction in hypoxia, which leads to the disassembling of block polymers. This disintegrates the polymersomes and releasing the encapsulated drugs [36] (Figure 3A).

To check the drug release from polymersomes, targeted DOX-loaded polymersomes (DOX-iPs) were prepared. The release behavior was evaluated within hypoxic and normoxic conditions as a function of time (Figure 3B).

The polymersomes released a significantly higher amount of Dox in hypoxia than normoxia. Polymersomes released about 95% of their encapsulated DOX in hypoxic conditions and about 25% in the normoxic condition in 12 hours. This confirmed that nanoparticles released their cargo due to the reduction of diazobenzene linker in hypoxia (Figure 3A).

AFM and TEM images showed that the nanoparticles' vesicular shape changed within hypoxia (Figure 4). Irregular morphology of the polymersomes in hypoxic conditions demonstrates possible disintegration and fusion of the polymeric vesicles (Figure 4B, 4D). We also observed that hypoxia decreased the hydrodynamic diameter and increased the vesicles' polydispersity index (Table 1).

3.3. Neuropilin-1 expression

To investigate any hypoxia-induced expression of NRP-1, the MDA-MB-231 cells grew under both normoxic (21% oxygen) and hypoxic (2% oxygen) conditions. Western blotting demonstrated a significant increase in NRP-1 protein expression within the cells cultured in hypoxia than normoxia (Figure 5). The protein β-actin used as an internal control. We found that the level of NRP-1 expression significantly increased after 24 hours within hypoxia

(Figure 5B). This result suggested that hypoxia might structurally and functionally induce transmembrane NRP-1 protein expression through angiogenesis in TNBC cells.

3.4. Cellular uptake

To demonstrate the nanoparticle penetration into TNBC cells, DPPE-lissamine rhodamine lipid (5%) was incorporated into the composition of polymersomes (without drug) to ease visualization fluorescence microscopic imaging.[23,37] The MDA-MB-231 cells were treated for 3 hours with both targeted and non-targeted polymersomes. The red fluorescence (lissamine rhodamine dye) was observed inside the cells treated with targeted nanoparticles under hypoxia. However, the cells incubated with non-targeted vesicles (control) did not show significant intensity of the red fluorescence inside the cells (Figure 6A) either in hypoxia or normoxia. The images' quantitative fluorescence integral density indicated a significant difference between the iRGD-targeted polymersomes in hypoxia and normoxia. The uptake results were significantly different for targeted and non-targeted polymersomes within hypoxia and normoxia (Figure 6B). It was found that the intensity of targeted nanoparticles was 8.5 times more than non-targeted polymersomes within the hypoxic condition and 3 times more than targeted nanoparticles within the normoxic condition. According to earlier studies, nanocarrier uptake in TNBC cells increases dynamically within the hypoxic condition.[38] Since TNBC cells overexpress the NRP-1 receptor on the surface,[39] targeted iRGD-conjugated polymersomes will show increased uptake within these cells. Besides, western blotting of MDA-MB-231 cells displayed an increased expression of NRP-1 under hypoxia. Based on these findings, we concluded that exposing the MDA-MB231 cells to iRGD-conjugated polymersomes for three hours elevated the cellular uptake.

3.5. Polymer toxicity and monolayer cytotoxicity

To assess polymer toxicity, the cells were treated with different amounts of the polymersomes encapsulating HEPES buffer within hypoxia and normoxia for 3 days. The polymersomes demonstrated more than 88% cell viability with a maximum of 100 μg/mL polymer concentration (Figure 7A), indicating minimal toxicity. To demonstrate polymersomes' efficacy, the MDA-MB-231 monolayer cultures were treated for 3 days using four groups: control (no treatment, HEPES buffer only), free drug, non-targeted, and targeted nanoparticles. The results demonstrated that incubating the MDA-MB-231 cells with 4 μM DOX encapsulated within targeted polymersomes under hypoxia reduced cell viability to 28% compared to normoxia (Figure 7B, $p < 0.05$). It was observed that targeted vesicles were more effective than non-targeted polymersomes and free DOX to kill TNBC cells under hypoxia. This is likely due to the binding of tumor-homing iRGD peptide on the targeted polymersomes with the overexpressed NRP-1 receptors on TNBC cells. According to drug release study (Figure 3B), nanoparticles released one-third (33%) of their loaded DOX within 3 h and around 79% within 8 h. Therefore, 3-day treatment will ensure enough time for the polymersomes to translocate the breast cancer cells, break open, and release their drug cargo within the cells.

3.6. Cell viability in spheroid cultures

The MDA-MB-231 three-dimensional spheroids were cultured for 3 days in hypoxic and normoxic conditions with the same treatment groups as a monolayer cell viability study

(Figure 8A). The results indicated that under hypoxia, the cell viability was significantly diminished to 36% when the spheroids were incubated with 4 μM DOX loaded within targeted vesicles in contrast to non-targeted vesicles within the normoxic condition (66%) (Figure 8B). However, there was no significant difference in viability when the cells were incubated with non-targeted vesicles or free drug within hypoxic and normoxic conditions. This might reflect the slow diffusion of non-targeted nanoparticles and DOX inside the three-dimensional cultures. Instead, targeted polymersomes showed enhanced cytotoxicity based on receptor-mediated cell penetration. Some polymersomes might release the encapsulated DOX in the extracellular regions. In this regard, the free drug penetrates the cells via the cell membrane.[40] However, passive diffusion could be less prevalent in comparison with targeted drug-encapsulated nanoparticle delivery.

3.7. *In vivo* anti-tumor efficacy

To evaluate the anti-tumor efficacy, MDA-MB-231 tumor-bearing female nude mice were administered through the tail vein with saline (control), DOX, plain polymersomes, non-targeted, and targeted DOX-polymersomes twice per week for 4 weeks. Mice were monitored daily for the drugs' potential toxicity, and the tumor volume and body weight were calculated once every three days. The percent tumor volume growth within days was calculated (Figure 9A) and suggested tumor growth inhibition in all DOX-treated groups compared to the control. The tumor growth in the group treated with plain polymersomes demonstrated a slight difference compared to the saline group. Free DOX showed an increase of 337% in tumor volume. Non-targeted polymersomes exhibited a 253% increase in tumor volume that was significantly different compared to the saline group. However, targeted DOX-encapsulated nanoparticles demonstrated a much lower growth in the volume (129%) and displayed a significant difference in comparison with non-targeted vesicles, DOX, and saline ($p < 0.05$ vs. non-targeted polymersomes $p < 0.01$ vs. free DOX, and $p < 0.001$ vs. saline). This suggested that targeted polymersomes were the most effective nanoparticles to inhibit TNBC tumor growth. After six weeks, we euthanized the animals, removed and weighed the tumors (Figure 9B).

The plain polymersomes, free DOX, and non-targeted polymersome treatment groups revealed the average tumor weights of 0.712, 0.661, and 0.565 g, respectively. However, the targeted polymersome treatment group resulted in the lowest average tumor weight of 0.312 g, significantly different compared to DOX treated groups and saline ($p < 0.05$ vs. non-targeted, $p < 0.01$ vs. free DOX, and $p < 0.001$ vs. saline). The percent tumor growth inhibition (TGI) was determined based on DOX treated groups' tumor volume compared to the saline tumor volume group (Figure 9C). The free DOX and non-targeted polymersome groups presented TGI of 41% and 55.7%, respectively. However, targeted polymersome treatment groups demonstrated a TGI of 77.6% that was significantly higher than non-targeted polymersome and free DOX treatment groups. Excised tumors in all treatment groups were dissected in half and imaged (Figure 9D). Overall, the expected high anti-tumor efficacy of the targeted polymersomes might be due to the defective tumor vasculature, enhanced blood circulation and accumulation within the tumors via surface-modified tumor penetrating iRGD peptide,[36] disintegration within hypoxic niches of breast tumors based on the presence of hypoxia-responsive moiety, and liberation of the drug within the cells.

3.8. *In vivo* toxicity of polymersomes

To determine the polymersomes' toxicity, main organs (lung, liver, and kidney) were collected at the end of the experiment and evaluated using histological assessments (hematoxylin and eosin staining, Figure 10). Histological analyses of mice treated with saline demonstrated some metastatic lesions within the liver tissue (black arrows) due to the diffusion of neoplastic cells through the vessels. The mice treated with DOX, non-targeted, and targeted nanoparticles did not show any metastatic lesion or toxicity. This presented substantial tumor growth inhibition and anti-tumor efficacy of the polymersome formulations and free drug. We did not evaluate heart tissue lesions in our study. However, possible toxicity might be expected with high doses of DOX to create myocardial damaged fibers. Overall, most of the organs treated with DOX-loaded vesicles were normal with no tissue necrosis or cell lesion. The histological evaluations demonstrated that non-targeted and targeted polymersomes delivered their drug cargo into the tumor tissues, enhanced anti-tumor efficacy, and reduced off-target toxicity.

3.9. Biodistribution and nanoparticle accumulation

To assess the biodistribution of the targeted polymersomes, fluorescently labeled iRGD-conjugated polymersomes were injected via the tail vein into the female nude mice. The mice were euthanized at predetermined time points, and the liver, kidney, and lung were excised and imaged (Figure 11A). We did not observe any significant polymersome accumulation within organs after either 3 h or 8 h post-injection. The biodistribution study showed that targeted nanoparticles might selectively accumulate within the tumor tissues and reduce off-target organ cytotoxicity. The fluorescence integral density of nanoparticle accumulation within organ tissues was calculated by NIH ImageJ software (Figure 11B).

4. Conclusion

We synthesized an amphiphilic diblock copolymer with a hypoxia-responsive diazobenzene linker capable of self-assembly into polymersomes. Doxorubicin was successfully encapsulated into the polymersomes. The tumor-targeting and penetrating iRGD peptide was conjugated into the polymersomes via click chemistry to make targeted hypoxia-responsive polymersomes. Targeted polymersomes exhibited higher cytotoxicity on TNBC cells in hypoxia than normoxia in monolayer and three-dimensional spheroid cell cultures. *In vivo* studies on TNBC tumor-bearing, nude mice demonstrated that targeted polymersomes had enhanced anti-tumor efficacy compared to non-targeted polymersomes and free doxorubicin. These drug-loaded polymer nanoparticles demonstrated no toxicity against various internal organs, such as the liver, kidney, and lung. This is the first administration of hypoxia-responsive iRGD-polymersomes encapsulating doxorubicin in animal models of triple-negative breast cancer. An earlier study has demonstrated tumor suppression by employing doxorubicin within hypoxia-responsive nanoparticles to reach the TNBC tumors via the EPR effect.[41] The nanoparticles in our study are hypoxia-responsive and iRGD-conjugated. Hence, they offer the benefit of selective delivery of doxorubicin to TNBC tumors via active receptor-mediated targeting and enhanced penetration into the cells while lowering the off-target toxicity compared to passive tumor diffusion of nanoparticles or free drugs. The inclusion of diazobenzene hypoxia-responsive moiety contributes to the selective release of

chemotherapeutics within breast tumors' hypoxic niches. The results of this study indicated that targeted hypoxia-responsive polymersomes could be administered for effective anticancer drug delivery into solid tumors of TNBC.

Supplementary Material

Refer to Web version on PubMed Central for supplementary material.

Acknowledgments

SM and VS acknowledge the support from NIH (NIGMS) grants 2R01GM 114080 and U54 GM12872 and partial support from NSF EPSCoR Track-1 Cooperative Agreement OIA #1946202. Any opinions, findings, and conclusions or recommendations expressed in this material are those of the author(s) and do not necessarily reflect the views of the NSF. Ms. Parinaz Ghanbari prepared the illustrations. SM and VS acknowledge support from the NIGMS COBRE award 1P20 GM109024 for the Animal Core Facility.

References

(1). Yan J; Liu Z; Du S; Li J; Ma L; Li L Diagnosis and Treatment of Breast Cancer in the Precision Medicine Era. Methods Mol Biol 2020, 2204, 53–61. 10.1007/978-1-0716-0904-0_5.

(2). Grobmyer SR; Zhou G; Gutwein LG; Iwakuma N; Sharma P; Hochwald SN Nanoparticle Delivery for Metastatic Breast Cancer. Nanomedicine: Nanotechnology, Biology and Medicine 2012, 8, S21–S30. 10.1016/j.nano.2012.05.011.

(3). Gold J; Winer EP Chemotherapy for Metastatic Breast Cancer. The Breast: Comprehensive Management of Benign and Malignant Disease 2009, 1233–1261.

(4). Mehanna J; Haddad FG; Eid R; Lambertini M; Kourie HR Triple-Negative Breast Cancer: Current Perspective on the Evolving Therapeutic Landscape. Int J Womens Health 2019, 11, 431–437. 10.2147/IJWH.S178349. [PubMed: 31447592]

(5). Dawson SJ; Provenzano E; Caldas C Triple Negative Breast Cancers: Clinical and Prognostic Implications. European Journal of Cancer 2009, 45, 27–40. 10.1016/S0959-8049(09)70013-9. [PubMed: 19775602]

(6). Lehmann BD; Bauer JA; Chen X; Sanders ME; Chakravarthy AB; Shyr Y; Pietenpol JA Identification of Human Triple-Negative Breast Cancer Subtypes and Preclinical Models for Selection of Targeted Therapies. J Clin Invest 2011, 121 (7), 2750–2767. 10.1172/JCI45014. [PubMed: 21633166]

(7). Lebert JM; Lester R; Powell E; Seal M; McCarthy J Advances in the Systemic Treatment of Triple-Negative Breast Cancer. Curr Oncol 2018, 25 (Suppl 1), S142–S150. 10.3747/co.25.3954. [PubMed: 29910657]

(8). Mamnoon B; Feng L; Froberg J; Choi Y; Sathish V; Mallik S Hypoxia-Responsive, Polymeric Nanocarriers for Targeted Drug Delivery to Estrogen Receptor-Positive Breast Cancer Cell Spheroids. Mol. Pharmaceutics 2020, 17 (11), 4312–4322. 10.1021/acs.molpharmaceut.0c00754.

(9). Gilkes DM; Semenza GL; Wirtz D Hypoxia and the Extracellular Matrix: Drivers of Tumour Metastasis. Nat Rev Cancer 2014, 14 (6), 430–439. 10.1038/nrc3726. [PubMed: 24827502]

(10). Hoffmann C; Mao X; Brown-Clay J; Moreau F; Absi AA; Wurzer H; Sousa B; Schmitt F; Berchem G; Janji B; Thomas C Hypoxia Promotes Breast Cancer Cell Invasion through HIF-1α-Mediated up-Regulation of the Invadopodial Actin Bundling Protein CSRP2. Sci Rep 2018, 8 (1), 1–14. 10.1038/s41598-018-28637-x. [PubMed: 29311619]

(11). Semenza GL The Hypoxic Tumor Microenvironment: A Driving Force for Breast Cancer Progression. Biochimica et Biophysica Acta (BBA) - Molecular Cell Research 2016, 1863 (3), 382–391. 10.1016/j.bbamcr.2015.05.036. [PubMed: 26079100]

(12). Liu J; Guo X; Luo Z; Zhang J; Li M; Cai K Hierarchically Stimuli-Responsive Nanovectors for Improved Tumor Penetration and Programed Tumor Therapy. Nanoscale 2018, 10 (28), 13737–13750. 10.1039/C8NR02971G. [PubMed: 29992216]

(13). Cuenca AG; Jiang H; Hochwald SN; Delano M; Cance WG; Grobmyer SR Emerging Implications of Nanotechnology on Cancer Diagnostics and Therapeutics. Cancer 2006, 107 (3), 459–466. 10.1002/cncr.22035. [PubMed: 16795065]

(14). Shi J; Kantoff PW; Wooster R; Farokhzad OC Cancer Nanomedicine: Progress, Challenges and Opportunities. Nature Reviews Cancer 2017, 17 (1), 20–37. 10.1038/nrc.2016.108. [PubMed: 27834398]

(15). Thambi T; Deepagan VG; Yoon HY; Han HS; Kim S-H; Son S; Jo D-G; Ahn C-H; Suh YD; Kim K; Chan Kwon I; Lee DS; Park JH Hypoxia-Responsive Polymeric Nanoparticles for Tumor-Targeted Drug Delivery. Biomaterials 2014, 35 (5), 1735–1743. 10.1016/j.biomaterials.2013.11.022. [PubMed: 24290696]

(16). Kozlovskaya V; Liu F; Xue B; Ahmad F; Alford A; Saeed M; Kharlampieva E Polyphenolic Polymersomes of Temperature-Sensitive Poly(N-Vinylcaprolactam)-Block-Poly(N-Vinylpyrrolidone) for Anticancer Therapy. Biomacromolecules 2017, 18 (8), 2552–2563. 10.1021/acs.biomac.7b00687. [PubMed: 28700211]

(17). Confeld MI; Mamnoon B; Feng L; Jensen-Smith H; Ray P; Froberg J; Kim J; Hollingsworth MA; Quadir M; Choi Y; Mallik S Targeting the Tumor Core: Hypoxia-Responsive Nanoparticles for the Delivery of Chemotherapy to Pancreatic Tumors. Mol. Pharmaceutics 2020, 17 (8), 2849–2863. 10.1021/acs.molpharmaceut.0c00247.

(18). Kulkarni P; Haldar MK; You S; Choi Y; Mallik S Hypoxia-Responsive Polymersomes for Drug Delivery to Hypoxic Pancreatic Cancer Cells. Biomacromolecules 2016, 17 (8), 2507–2513. 10.1021/acs.biomac.6b00350. [PubMed: 27303825]

(19). Golombek SK; May J-N; Theek B; Appold L; Drude N; Kiessling F; Lammers T Tumor Targeting via EPR: Strategies to Enhance Patient Responses. Adv Drug Deliv Rev 2018, 130, 17–38. 10.1016/j.addr.2018.07.007. [PubMed: 30009886]

(20). Kulkarni P; Haldar MK; Katti P; Dawes C; You S; Choi Y; Mallik S Hypoxia Responsive, Tumor Penetrating Lipid Nanoparticles for Delivery of Chemotherapeutics to Pancreatic Cancer Cell Spheroids. Bioconjugate Chem. 2016, 27 (8), 1830–1838. 10.1021/acs.bioconjchem.6b00241.

(21). Niu S; Bremner DH; Wu J; Wu J; Wang H; Li H; Qian Q; Zheng H; Zhu L L-Peptide Functionalized Dual-Responsive Nanoparticles for Controlled Paclitaxel Release and Enhanced Apoptosis in Breast Cancer Cells. Drug Delivery 2018, 25 (1), 1275–1288. 10.1080/10717544.2018.1477863. [PubMed: 29847177]

(22). Miller-Kleinhenz JM; Bozeman EN; Yang L Targeted Nanoparticles for Image-Guided Treatment of Triple Negative Breast Cancer: Clinical Significance and Technological Advances. Wiley Interdiscip Rev Nanomed Nanobiotechnol 2015, 7 (6), 797–816. 10.1002/wnan.1343. [PubMed: 25966677]

(23). Karandish F; Mamnoon B; Feng L; Haldar MK; Xia L; Gange KN; You S; Choi Y; Sarkar K; Mallik S Nucleus-Targeted, Echogenic Polymersomes for Delivering a Cancer Stemness Inhibitor to Pancreatic Cancer Cells. Biomacromolecules 2018, 19 (10), 4122–4132. 10.1021/acs.biomac.8b01133. [PubMed: 30169024]

(24). Guan L; Rizzello L; Battaglia G Polymersomes and Their Applications in Cancer Delivery and Therapy. Nanomedicine 2015, 10 (17), 2757–2780. 10.2217/nnm.15.110. [PubMed: 26328898]

(25). Martin C; Aibani N; Callan JF; Callan B Recent Advances in Amphiphilic Polymers for Simultaneous Delivery of Hydrophobic and Hydrophilic Drugs. Therapeutic Delivery 2015, 7 (1), 15–31. 10.4155/tde.15.84.

(26). Teesalu T; Sugahara KN; Ruoslahti E Tumor-Penetrating Peptides. Front Oncol 2013, 3. 10.3389/fonc.2013.00216.

(27). Kulkarni P; Haldar MK; Karandish F; Confeld M; Hossain R; Borowicz P; Gange K; Xia L; Sarkar K; Mallik S Tissue-Penetrating, Hypoxia-Responsive Echogenic Polymersomes For Drug Delivery To Solid Tumors. Chemistry – A European Journal 2018, 24 (48), 12490–12494. 10.1002/chem.201802229.

(28). Sugahara KN; Teesalu T; Karmali PP; Kotamraju VR; Agemy L; Girard OM; Hanahan D; Mattrey RF; Ruoslahti E Tissue-Penetrating Delivery of Compounds and Nanoparticles into Tumors. Cancer Cell 2009, 16 (6), 510–520. 10.1016/j.ccr.2009.10.013. [PubMed: 19962669]

(29). Krausz AE; Adler BL; Makdisi J; Schairer D; Rosen J; Landriscina A; Navati M; Alfieri A; Friedman JM; Nosanchuk JD; Rodriguez-Gabin A; Ye KQ; McDaid HM; Friedman AJ Nanoparticle-Encapsulated Doxorubicin Demonstrates Superior Tumor Cell Kill in Triple Negative Breast Cancer Subtypes Intrinsically Resistant to Doxorubicin. Precis Nanomed 2018, 1 (3), 173–182. 10.33218/prnano1(3).181029.1. [PubMed: 31032494]

(30). Gref R; Minamitake Y; Peracchia MT; Trubetskoy V; Torchilin V; Langer R Biodegradable Long-Circulating Polymeric Nanospheres. Science 1994, 263 (5153), 1600–1603. 10.1126/science.8128245. [PubMed: 8128245]

(31). Anajafi T; Yu J; Sedigh A; Haldar MK; Muhonen WW; Oberlander S; Wasness H; Froberg J; Molla MS; Katti KS; Choi Y; Shabb JB; Srivastava DK; Mallik S Nuclear Localizing Peptide-Conjugated, Redox-Sensitive Polymersomes for Delivering Curcumin and Doxorubicin to Pancreatic Cancer Microtumors. Mol. Pharmaceutics 2017, 14 (6), 1916–1928. 10.1021/acs.molpharmaceut.7b00014.

(32). Du Y; Chen W; Zheng M; Meng F; Zhong Z PH-Sensitive Degradable Chimaeric Polymersomes for the Intracellular Release of Doxorubicin Hydrochloride. Biomaterials 2012, 33 (29), 7291–7299. 10.1016/j.biomaterials.2012.06.034. [PubMed: 22795540]

(33). Krishnamachary B; Penet M-F; Nimmagadda S; Mironchik Y; Raman V; Solaiyappan M; Semenza GL; Pomper MG; Bhujwalla ZM Hypoxia Regulates CD44 and Its Variant Isoforms through HIF-1α in Triple Negative Breast Cancer. PLOS ONE 2012, 7 (8), e44078. 10.1371/journal.pone.0044078. [PubMed: 22937154]

(34). Liu X; Jiang J; Ji Y; Lu J; Chan R; Meng H Targeted Drug Delivery Using IRGD Peptide for Solid Cancer Treatment. Mol. Syst. Des. Eng. 2017, 2 (4), 370–379. 10.1039/C7ME00050B. [PubMed: 30498580]

(35). Patel A; Sant S Hypoxic Tumor Microenvironment: Opportunities to Develop Targeted Therapies. Biotechnology Advances 2016, 34 (5), 803–812. 10.1016/j.biotechadv.2016.04.005. [PubMed: 27143654]

(36). Confeld MI; Mamnoon B; Feng L; Jensen-Smith H; Ray P; Froberg J; Kim J; Hollingsworth MA; Quadir M; Choi Y; Mallik S Targeting the Tumor Core: Hypoxia-Responsive Nanoparticles for Delivery of Chemotherapy to Pancreatic Tumors. Mol. Pharmaceutics 2020. 10.1021/acs.molpharmaceut.0c00247.

(37). Mamnoon B; Feng L; Froberg J; Choi Y; Sathish V; Mallik S Hypoxia-Responsive, Polymeric Nanocarriers for Targeted Drug Delivery to Estrogen Receptor-Positive Breast Cancer Cell Spheroids. Mol. Pharmaceutics 2020, 17 (11), 4312–4322. 10.1021/acs.molpharmaceut.0c00754.

(38). Brownlee WJ; Seib FP Impact of the Hypoxic Phenotype on the Uptake and Efflux of Nanoparticles by Human Breast Cancer Cells. Scientific Reports 2018, 8 (1), 12318. 10.1038/s41598-018-30517-3. [PubMed: 30120388]

(39). Cano-Cortes MV; Navarro-Marchal SA; Ruiz-Blas MP; Diaz-Mochon JJ; Marchal JA; Sanchez-Martin RM A Versatile Theranostic Nanodevice Based on an Orthogonal Bioconjugation Strategy for Efficient Targeted Treatment and Monitoring of Triple Negative Breast Cancer. Nanomedicine: Nanotechnology, Biology and Medicine 2020, 24, 102120. 10.1016/j.nano.2019.102120.

(40). Dalmark M The Physicochemical Properties and Transmembraneous Transport of Doxorubicin. In Anthracycline Antibiotics in Cancer Therapy: Proceedings of the International Symposium on Anthracycline Antibiotics in Cancer Therapy, New York, New York, 16–18 September 1981; Muggia FM, Young CW, Carter SK, Eds.; Developments in Oncology; Springer Netherlands: Dordrecht, 1982; pp 165–172. 10.1007/978-94-009-7630-6_15.

(41). Zhang P; Yang H; Shen W; Liu W; Chen L; Xiao C Hypoxia-Responsive Polypeptide Nanoparticles Loaded with Doxorubicin for Breast Cancer Therapy. ACS Biomater. Sci. Eng. 2020, 6 (4), 2167–2174. 10.1021/acsbiomaterials.0c00125. [PubMed: 33455312]

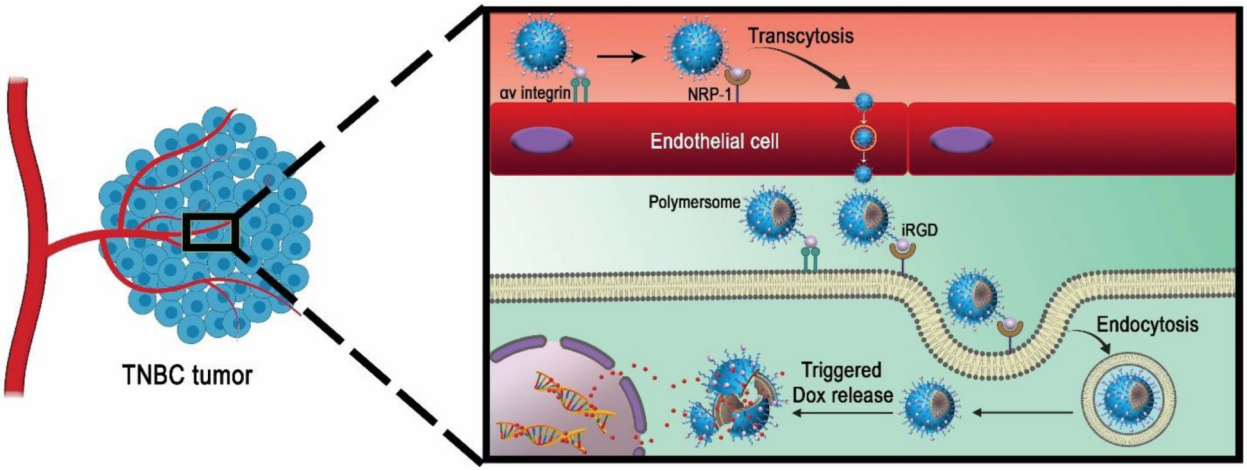

Figure 1.
Schematic illustration of the iRGD peptide-mediated targeting and penetration into the solid TNBC by the polymersomes.

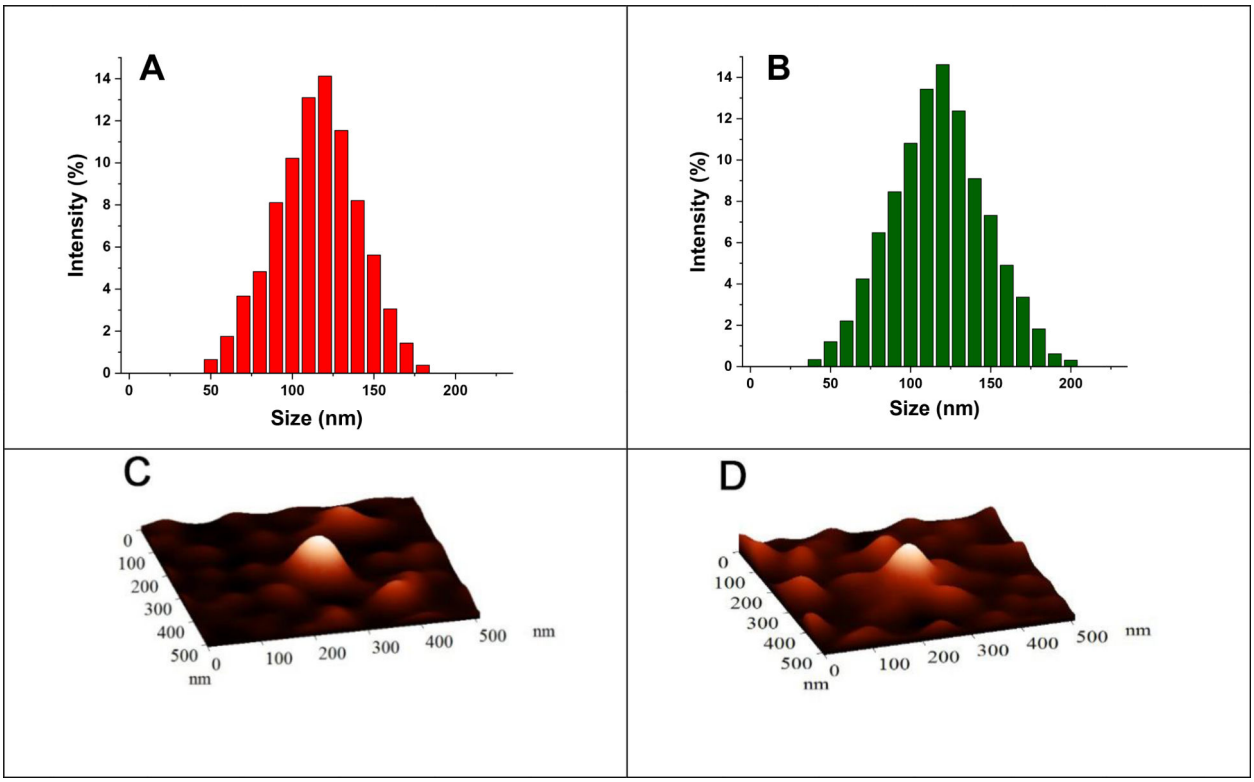

Figure 2.

The size of non-targeted (**A**) and targeted (**B**) nanoparticles. AFM images of non-targeted (**C**) and targeted (**D**) nanoparticles.

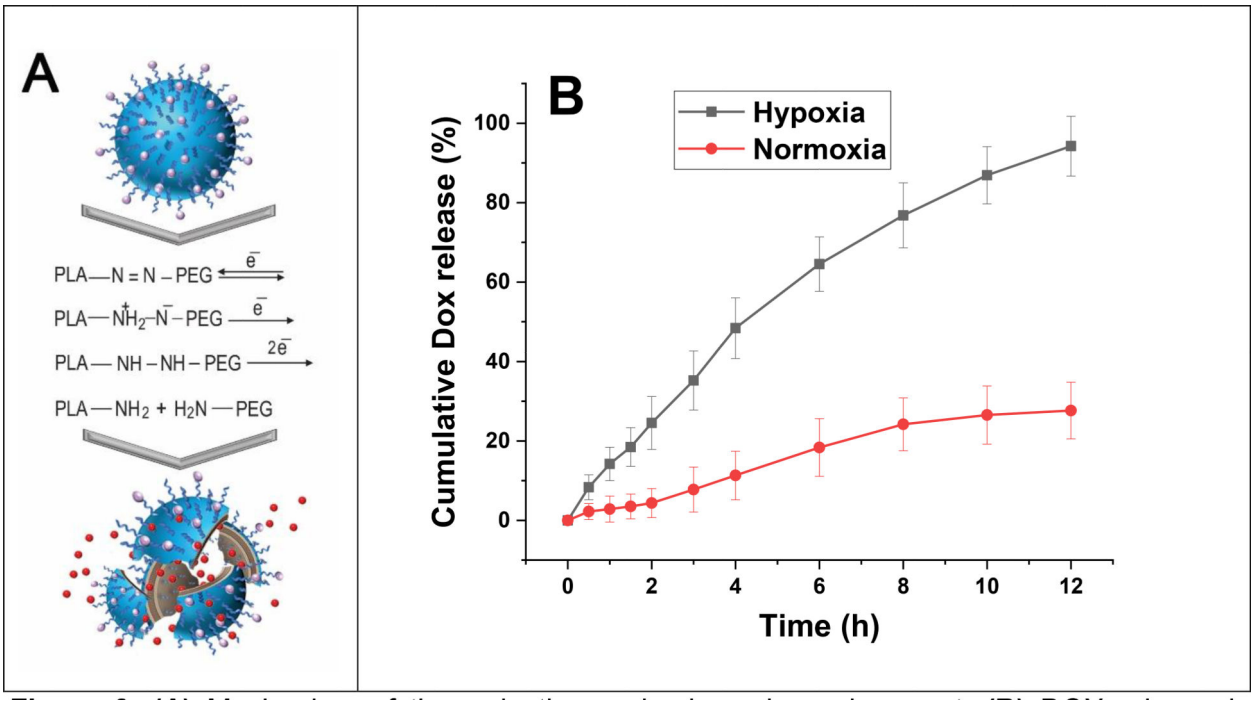

Figure 3.

(A) Mechanism of the reduction under hypoxic environment. **(B)** DOX release in hypoxic (2% oxygen) and normoxic (21% oxygen) conditions (n = 3).

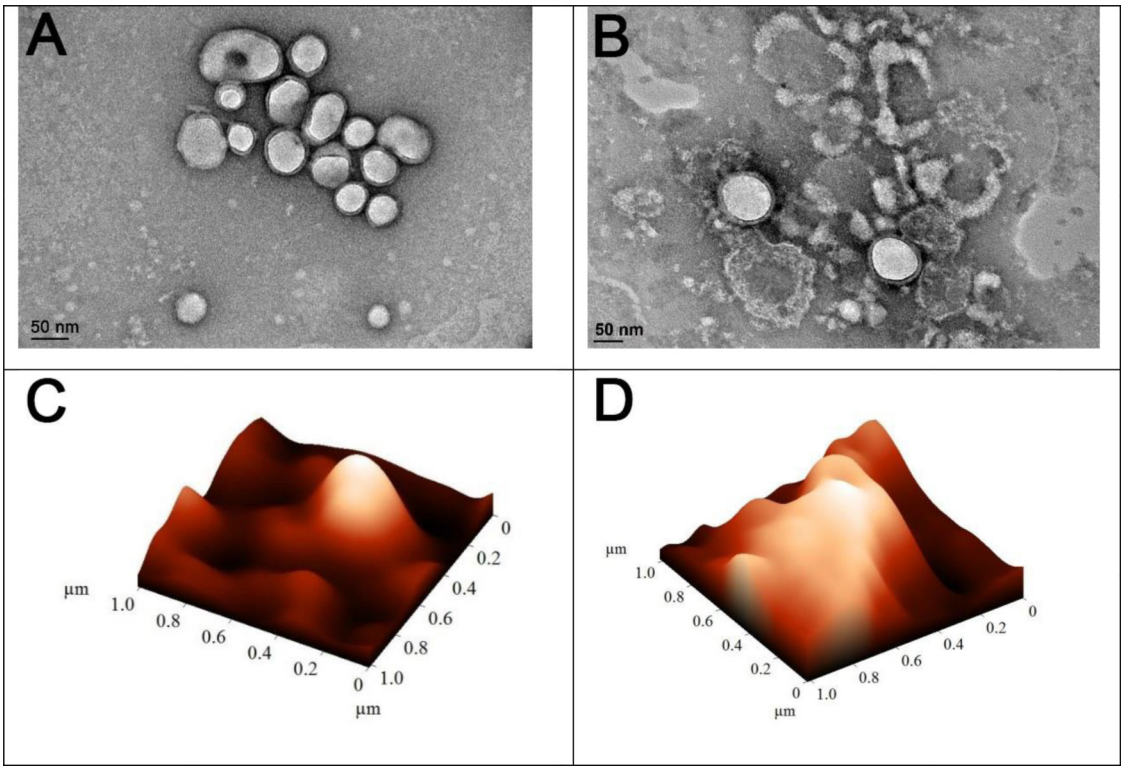

Figure 4.

AFM and TEM images of the vesicles within normoxic (**A**, **C**) and hypoxic (**B**, **D**) conditions (scale bar: 50 nm).

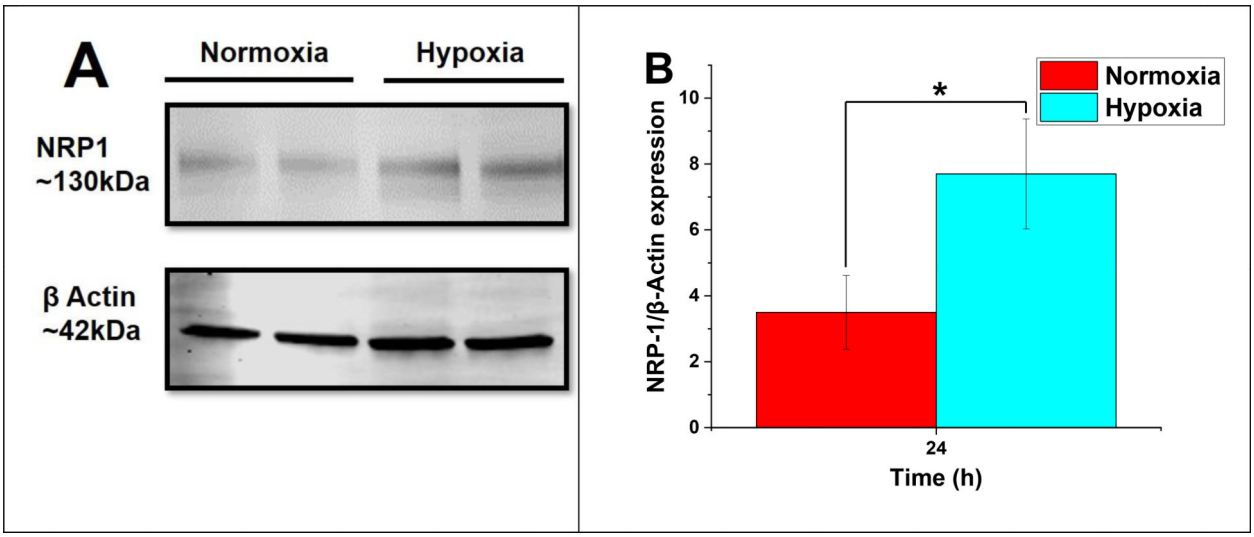

Figure 5.

(A) NRP-1 expression in MDA-MB-231 cells with significant upregulation in hypoxic conditions (24h exposure). (**B**) The level of NRP-1/β-Actin expression (n = 3, *p < 0.05).

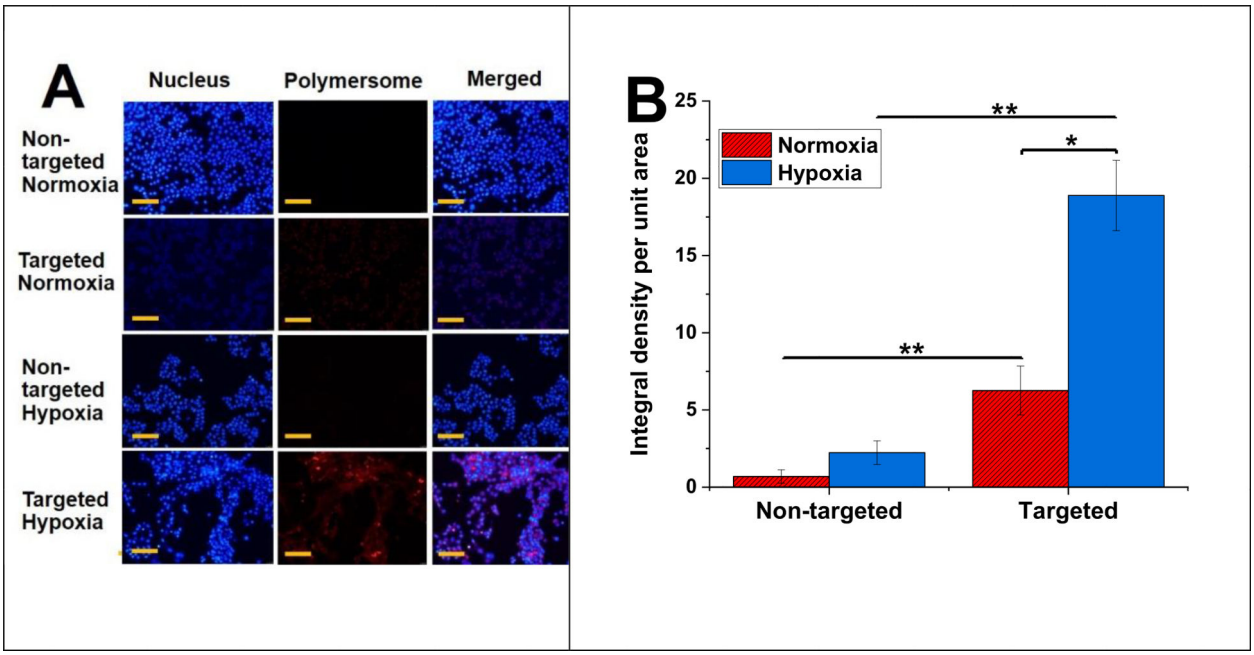

Figure 6.

(A) Fluorescence microsocpic images of polymersome uptake in MDA-MB-231 cells under hypoxia and normoxia (scale bar: 50 μm). **(B)** Image intensity of polymersome uptake (n = 3, *p < 0.05, **p < 0.01).

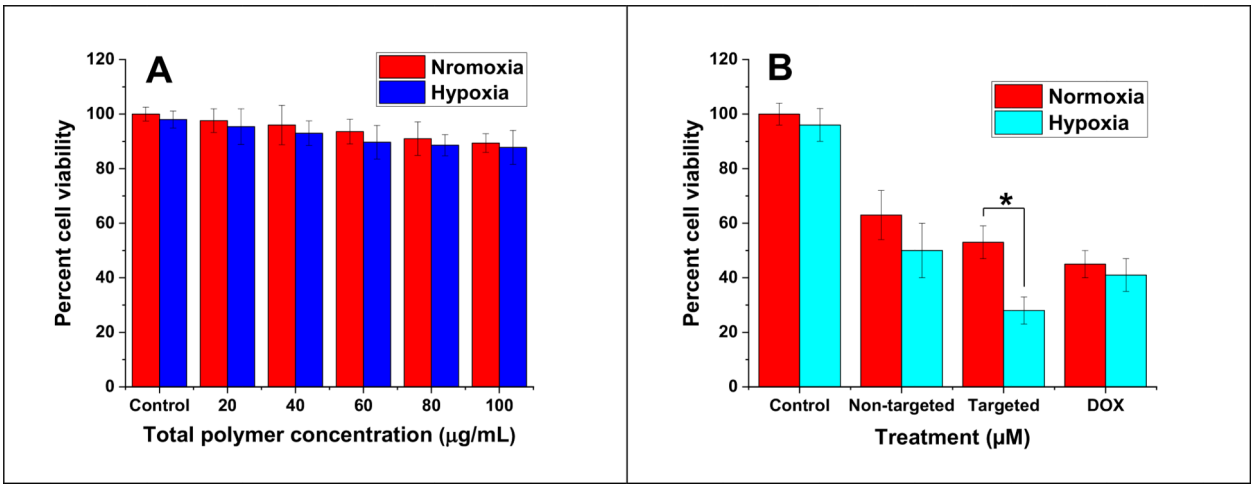

Figure 7.

Viability of MDA-MB-231 cells (monolayer) after 3-day treatment with buffer-encapsulated polymersomes (**A**, n = 6), free DOX, non-targeted, and targeted polymersomes (**B**, n = 3, * P < 0.05).

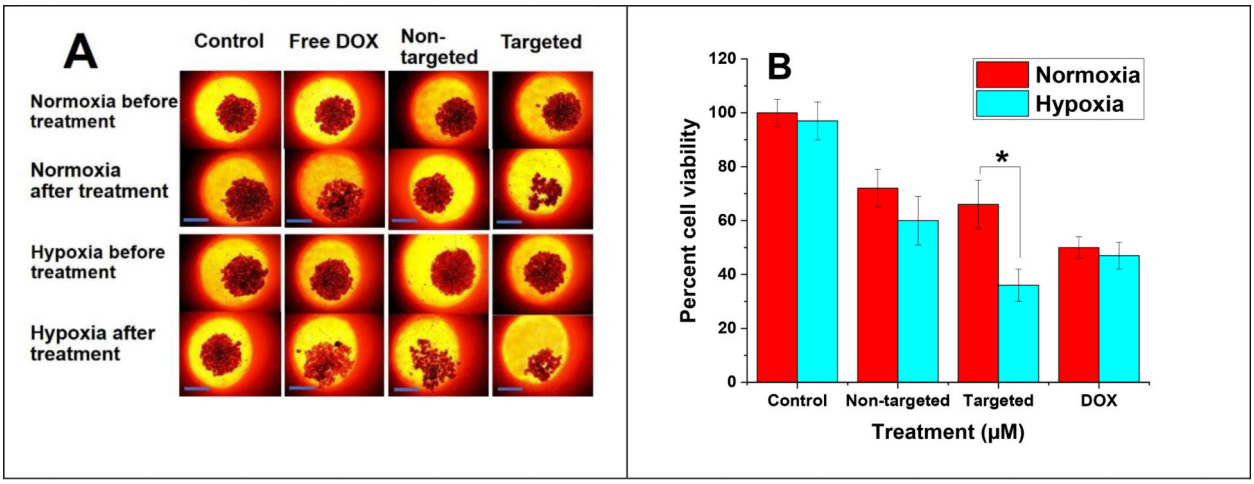

Figure 8.

(A) Three-dimensional MDA-MB-231 spheroid images before and after incubating the cells with non-targeted and targeted vesicles under hypoxic and normoxic conditions (scale bar: 100 μm). **(B)** Viability of MDA-MB-231 cell spheroids (n = 3, * P < 0.05).

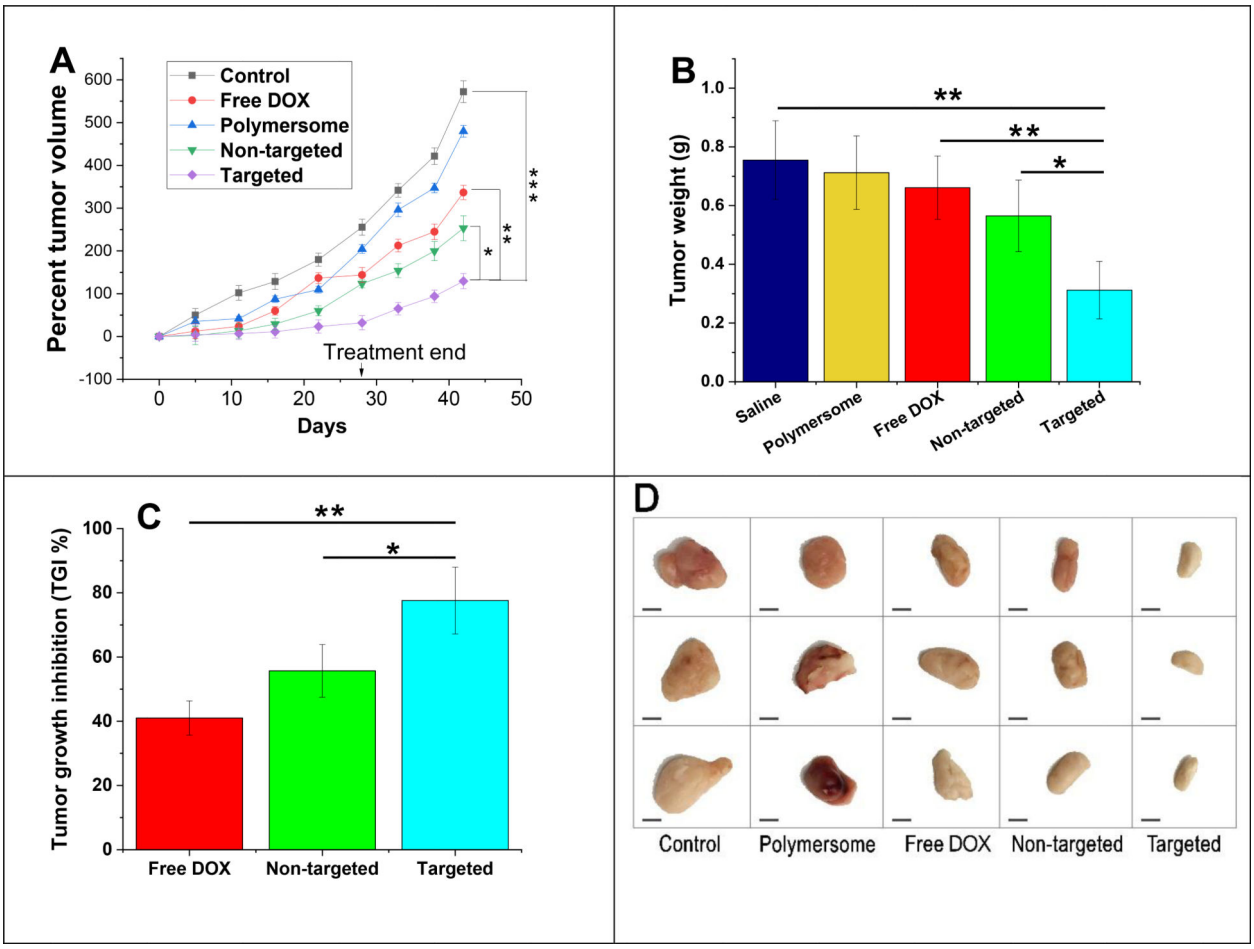

Figure 9.

In vivo anti-tumor efficacy studies **(A)** Tumor volume growth of MDA-MB-231 cancer xenografts treated with saline, plain polymersomes, DOX, targeted, and non-targeted polymersomes with a dose of 5 mg DOX/kg. **(B)** Average tumor weight of all treatment groups (n = 3, *p < 0.05, **p < 0.01). **(C)** Percent tumor growth inhibition (TGI) of DOX treated groups (n = 3, *p < 0.05, **p < 0.01). **(D)** Excised tumor images from outside (scale bar: 5 mm).

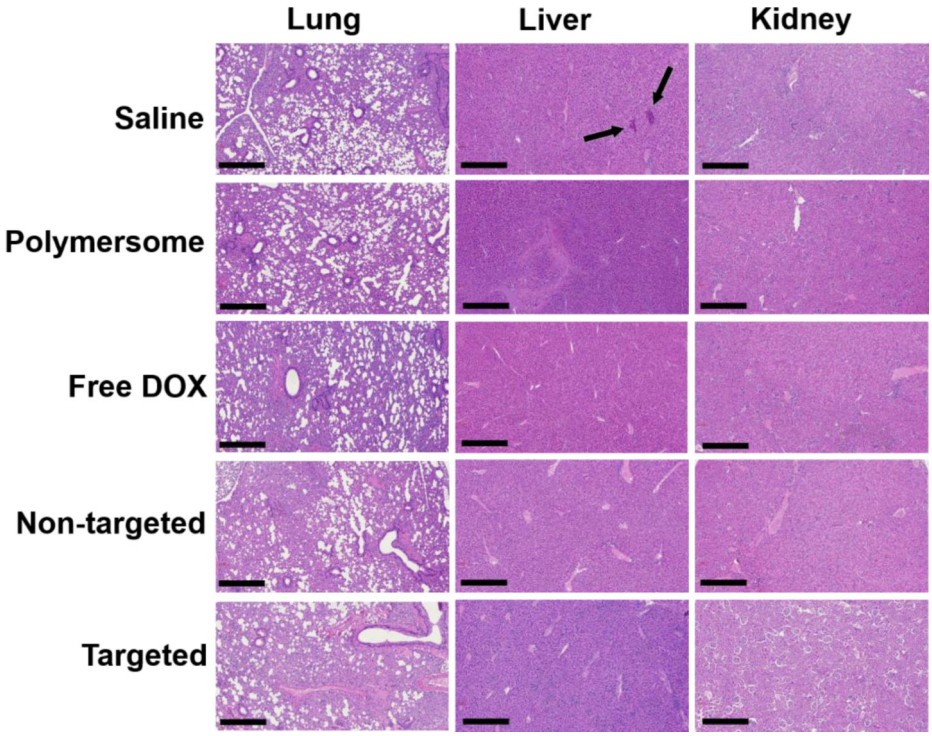

Figure 10.

Histological assessment of lung, liver, and kidney tissues of nude mice after treating with control, free DOX, non-targeted, targeted, and plain polymersomes (scale bar: 100 μm,10x objective). In the saline-treated group, liver tissues demonstrated metastatic lesions (black arrows).

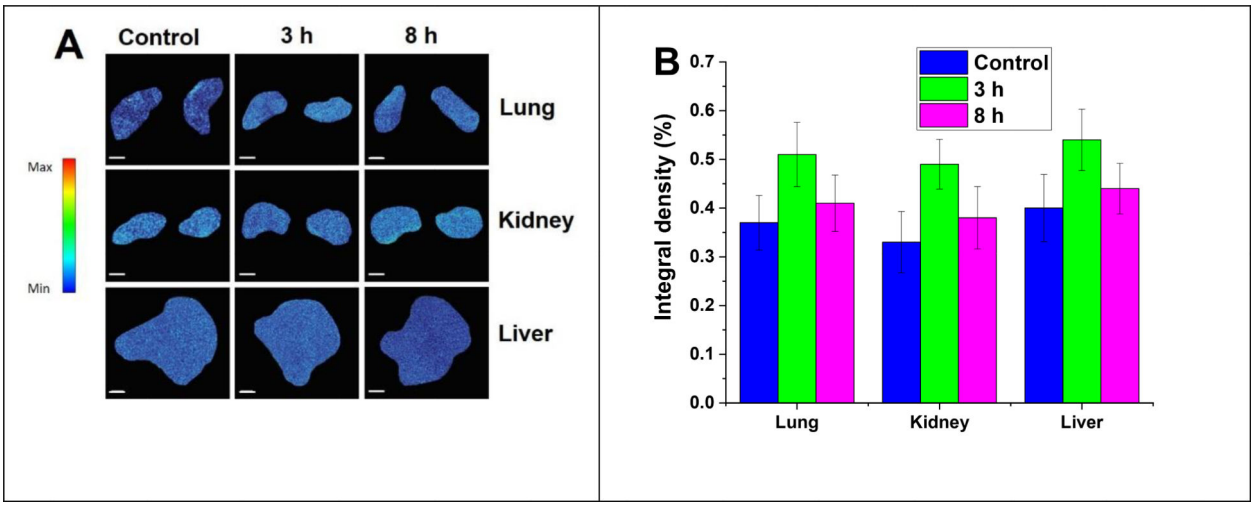

Figure 11.

(A) Biodistribution to organs at 3 h and 8 h post-injection of indocyanine green-loaded iRGD-polymersomes (n = 3) (scale bar: 2 mm). **(B)** Accumulation of targeted Polymersomes in organs after 3 h and 8 h post-injection of polymersomes (n = 3).

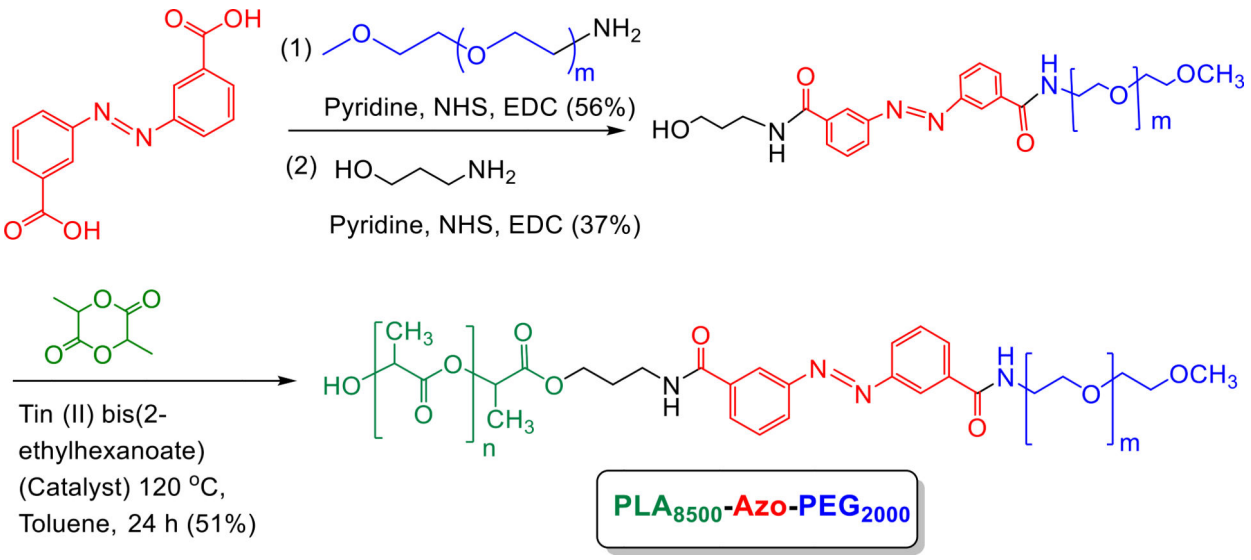

Scheme 1.

Synthesis of the polymer with hypoxia-sensitive diazobenzene linker (green: PLA; red: hypoxia-responsive linker; blue: PEG).

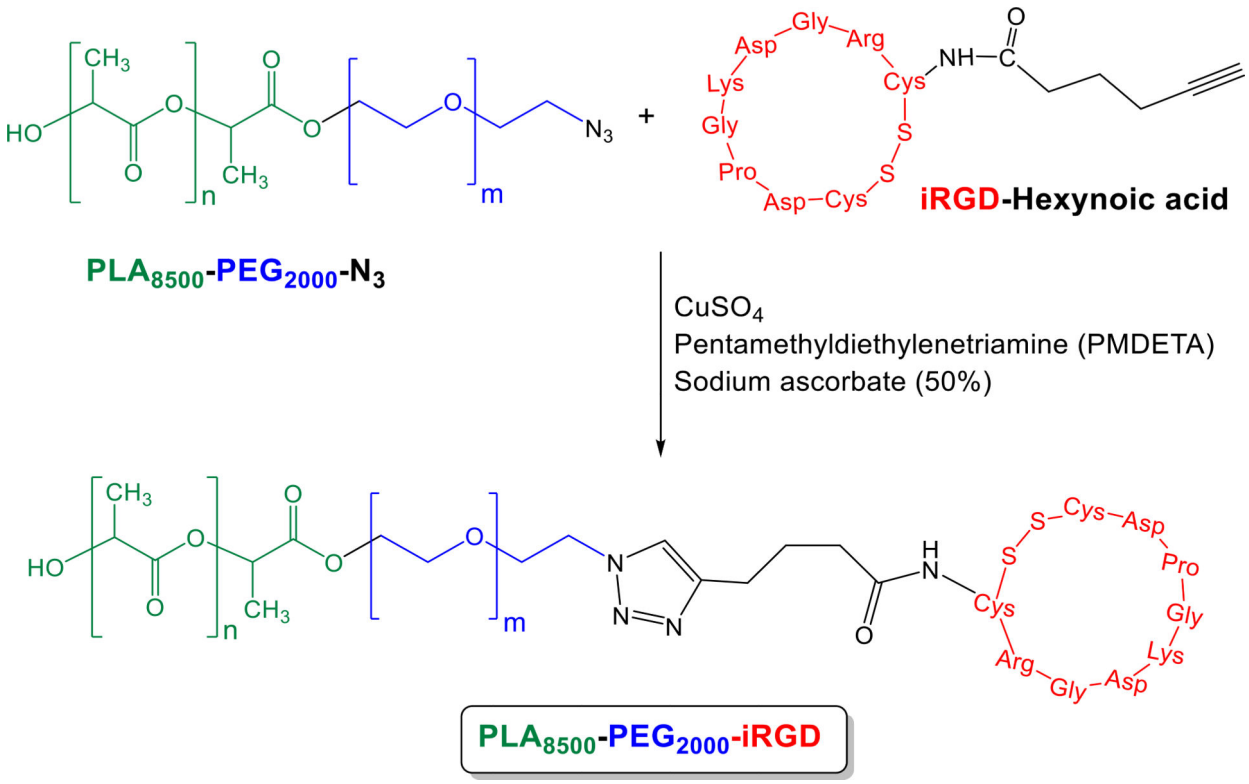

Scheme. 2.

Reaction of PLA_{8500}–PEG_{2000}–N_3 polymer and Hex-iRGD.

Table 1.

Diameter, ζ potential, and PDI of different polymersomes.

Polymersome	Average diameter (nm)		ζ potential (mV)		PDI	
	Normoxia	Hypoxia	Normoxia	Hypoxia	Normoxia	Hypoxia
Non-targeted	118 ± 4	43 ± 4, 419 ± 22	0.13 ± 0.09	0.21 ± 0.11	0.13 ± 0.02	0.73 ± 0.16
Targeted	136 ± 7	51 ± 3, 574 ± 27	0.23 ± 0.12	0.31 ± 0.14	0.18 ± 0.05	0.76 ± 0.19